THE JOURNAL OF PHYSICAL CHEMISTRY B

Article

pubs.acs.org/JPCB

Catalytic Mechanism and Product Specificity of Oxidosqualene-Lanosterol Cyclase: A QM/MM Study

Bo-Xue Tian[†] and Leif A. Eriksson[‡,*]

[†]School of Chemistry, National University of Ireland—Galway, Galway, Ireland

[‡]Department of Chemistry and Molecular Biology, University of Gothenburg, 412 96 Göteborg, Sweden

Supporting Information

ABSTRACT: Oxidosqualene-lanosterol cyclase (OSC) is a key enzyme in the biosynthesis of cholesterol. The catalytic mechanism and the product specificity of OSC have herein been studied using QM/MM calculations. According to our calculations, the protonation of the epoxide ring of oxidosqualene is rate-limiting. Wild-type OSC (which generates lanosterol), and the mutants H232S (which generates parkeol) and H232T (which generates protosta-12,24-dien-3-β-ol) were modeled, in order to explain the product specificity thereof. We show that the product specificity of OSC at the hydride/methyl-shifting stage is unlikely to be achieved by the stabilization of the cationic intermediates, as the precursor of lanosterol is in fact not the most stable cationic intermediate for wild-type OSC. The energy barriers for the product-determining conversions are instead found to be related to the product specificity of different OSC mutants, and we thus suggest that the product specificity of OSC is likely to be controlled by kinetics, rather than thermodynamics.

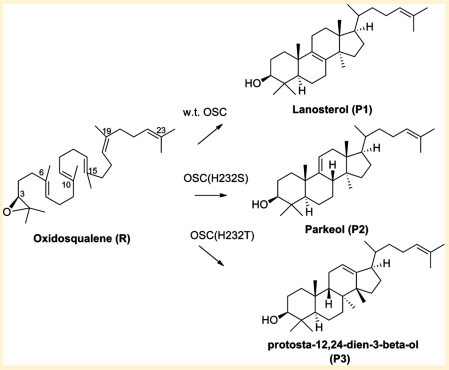

INTRODUCTION

Oxidosqualene-lanosterol cyclase (OSC), which catalyzes the conversion from oxidosqualene to lanosterol, is a key enzyme in the biosynthesis of cholesterol.[1] OSC inhibitors are drug candidates against hypercholesterolemia.[2−4] The proposed catalytic mechanism of OSC is shown in Scheme 1.[3] Protonation of the epoxide ring of oxidosqualene by Asp455 triggers ring-forming reactions, yielding the protosterol cation **4**. A series of 1,2-hydride and 1,2-methyl group shifts then occur, followed by a final deprotonation step leads to the product lanosterol (Scheme 1).[3] In the crystal structure of the OSC-lanosterol complex, His232 and Tyr503 (human OSC numbering) are in favorable positions for the final deprotonation step (Scheme 2).[3] Mutation of the active site histidine His232 to different amino acids leads to diverse products, some of which are shown in Scheme 2.[5]

Although multiple cationic/olefin intermediates are formed during the catalytic process of wild type OSC, the sole product lanosterol is obtained. We divide the OSC specificity into two stages, i.e., before or after the formation of protosterol cation **4**. In the first stage, the 4-ring chair−boat−chair scaffold protosterol cation is the dominant intermediate formed in wild-type OSC, while various byproducts from 1-ring to 3-ring are observed in OSC mutants.[5−14] In the second stage, although the hydride and methyl shifts may results in many different 4-ring products (e.g., P1, P2, and P3; Scheme 2), only lanosterol is formed in wild-type OSC.

To date, no computational study on the overall mechanism of OSC has been reported, except that the first step (conversion **R**→**1**) was studied by QM calculations on small models.[15] The mechanism of squalene-hopene cyclase (SHC), a closely related enzyme, has been investigated in a number of computational studies,[16−23] where the ring formation steps have been discussed in great detail. In the current work, we are interested in the product specificity at the hydride/methyl-shifting stage, which was never previously studied. In particular, two representative mutants were considered, i.e. H232S and H232T, which generate sole product Parkeol (**P2**) and protosta-12,24-dien-3-β-ol (**P3**), respectively (Scheme 2).[5]

COMPUTATIONAL DETAILS

DFT Calculations. The DFT functionals B3LYP[24−26] and M06−2X[27] were used to study the energies of the key intermediates and products. Geometries were optimized in vacuo using B3LYP with the 6-31G(d) basis set (BS1), followed by frequency calculations at the same level of theory. Single-point energy calculations were performed on the optimized structures using the higher basis set 6-311+G(2d,p) (BS2). All DFT calculations were performed using the Gaussian 09 program.[28]

ONIOM Calculations. The crystal structure of the OSC−lanosterol complex (PDB code 1W6K[3]) was obtained from the RCSB Protein Data Bank. Hydrogen atoms were added using the Molecular Operating Environment (MOE) software (Version 2010.10).[29] Lanosterol, Asp455, Tyr503, and His232 were included in the QM region in the QM/MM calculations.

Received: September 14, 2012
Revised: November 5, 2012
Published: November 6, 2012

   dx.doi.org/10.1021/jp3091396 | J. Phys. Chem. B 2012, 116, 13857−13862

Scheme 1. Proposed Mechanism of OSC[3]

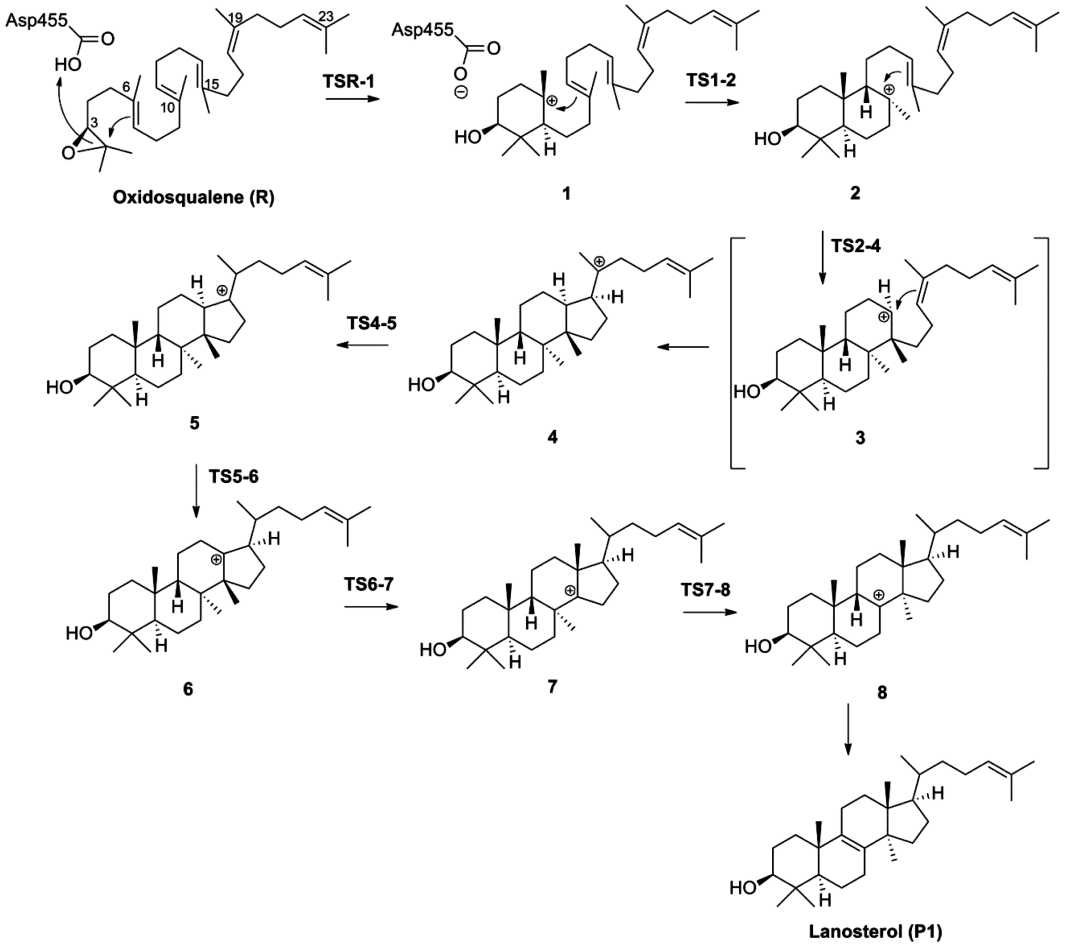

In the OSC−lanosterol complex, Asp455 was set to the deprotonated form, and Tyr503 was set to the protonated form (in the corresponding reactant complex, Asp455 is protonated and Tyr503 is deprotonated, cf. Scheme 1). Three different protonation states for His232 were considered in the wild-type OSC, i.e., HID, HIE, and HIP (the HID model is shown in Scheme 2, which is favored in the MOE protonation 3D prediction, the other models are shown in Supporting Information S1). It should be noted that HID232 might be the base for the deprotonation step in wild-type OSC, but in the two mutants in Scheme 2, Tyr503 is the only base suitable for deprotonation. As the deprotonation by Tyr503 is easier than that by HID232 (data not shown), we only discuss the Tyr503 residue as the base for deprotonation. Intermediates and TSs in the proposed mechanism (Scheme 1) from the product complex (OSC−lanosterol) to the reactant complex (OSC−oxidosqualene) were optimized using wild-type OSC (HID form). Key intermediates **6**−**9** were then optimized using the H232S and H232T mutants, as well as HIE and HIP forms of wild type OSC. The mutants were built using a similar approach as previously reported.[30]

The ONIOM method[31] was used for all QM/MM optimizations. The systems were initially optimized using the AMBER 03 force field.[32] Missing parameters of lanosterol were derived using Antechamber[33,34] with the RESP charge method (Supporting Information S2). A two-layer ONIOM (QM/MM) scheme with electronic embedding (EE) was used. Geometries were optimized at the ONIOM-EE (B3LYP/BS1:AMBER) level. Atoms far away from the lanosterol atoms (>10 Å) were held fixed during the QM/MM optimizations. Frequency calculations were performed on the QM atoms only (using the "geom = readfreeze" option in G09) to confirm the correct normal modes of the imaginary frequency in those TSs. Full frequency calculations were not performed due to shortage of memory. Single-point energy calculations were performed on the optimized geometries with ONIOM-EE (B3LYP/BS2:AMBER). All ONIOM calculations were performed using the Gaussian 09 software.[28] It should be noted that our energy calculations are based on single snapshot QM/MM minimizations, thus the entropic contributions are not taken into account. Balancing accuracy and computational cost, the current methodology is a reasonable choice for modeling such a complex system, although one should be aware of its limitations.

RESULT AND DISCUSSION

DFT Calculations on Key Intermediates and Products.

The two DFT methods B3LYP and M06−2X were used to analyze the gas phase energies of the cation intermediates in Schemes 1 and 2, and the results are summarized in Table 1. Recently, Kürti et al.[16] studied the energies of various cations involved in the OSC catalysis using quantum mechanics calculations. They suggest that OSC utilizes a nonstop process, and that product specificity of OSC is probably achieved by the stabilization of the cationic intermediates.[16] According to their hypothesis, to selectively produce lanosterol, intermediate **8**

dx.doi.org/10.1021/jp3091396 | J. Phys. Chem. B 2012, 116, 13857−13862

Scheme 2. OSC Mutants and Their Corresponding Products

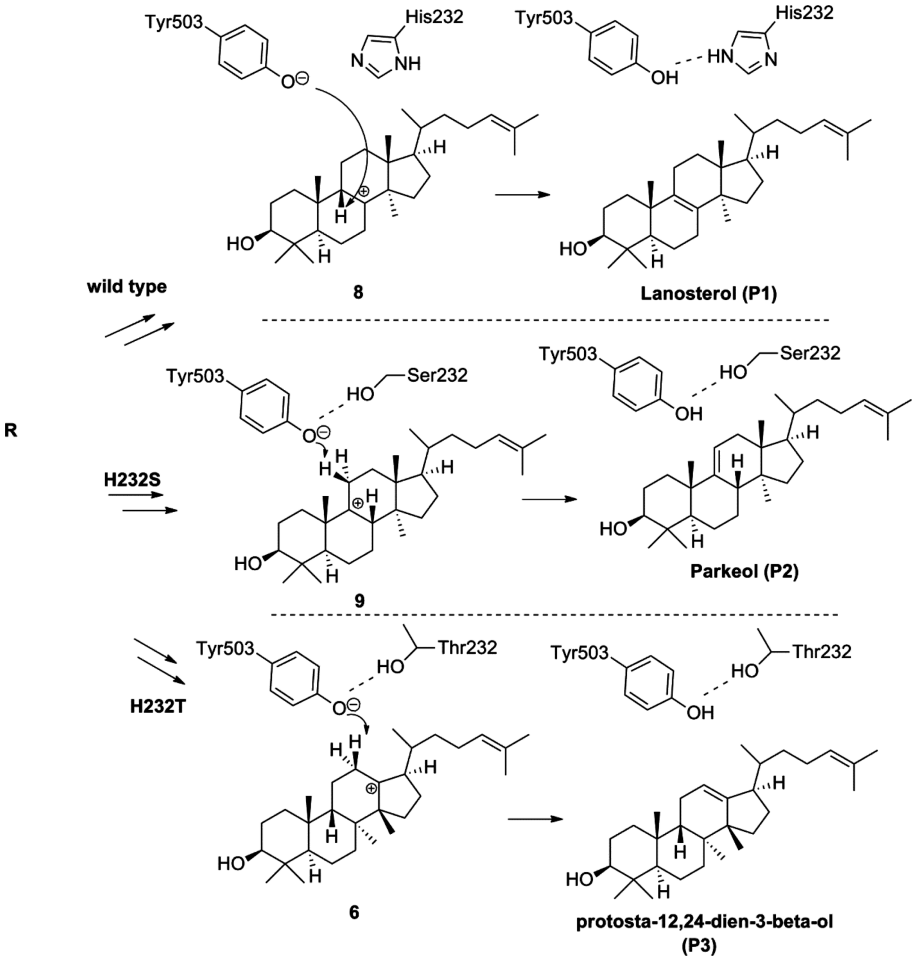

Table 1. Gas Phase Energies of Various Cation Intermediates

cationic intermediate[a]	E_{B3LYP}[b]	E_{M06-2X}[c]
1	0.0	0.0
2	−9.1	−22.3
4	−8.5	−36.3
5	−14.0	−41.3
6	**-16.8**	**-44.3**
7	−12.8	−40.6
8	**-15.3**	**-43.5**
9	**-17.2**	**-46.0**

[a]The structures of intermediates **1**−**9** are described in Schemes 1 and 2. [b]Relative energies at the B3LYP/BS2//B3LYP/BS1 level. [c]Relative energies at the M06−2X/BS2//B3LYP/BS1 level.

must have lower energy than **6** and **9** (Scheme 2). However, our DFT calculations disprove this, in that intermediate **8** is less stable than **6** or **9** in terms of gas phase energy (Table 1).

The gas phase energies of the three products in Scheme 2 were also compared (Table 2). According to our calculations, the energies of **P1** and **P3** are close, while **P2** seems to be thermodynamically much less stable. Taken together, the gas phase calculations on the key intermediates and products do not favor **P1** as the sole product. To investigate the product specificity of OSC, it thus appears that one must take the enzymatic environment into account, rather than simply look at the gas phase energies of the isolated intermediates.

Table 2. Gas Phase Energies of the Three Major Products

product[a]	E_{B3LYP}[b]	E_{M06-2X}[c]
P1	0.0	0.0
P2	11.8	11.6
P3	0.5	−1.0

[a]Product structures are described in Scheme 2. [b]Relative energies at the B3LYP/BS2//B3LYP/BS1 level. [c]Relative energies at the M06−2X/BS2//B3LYP/BS1 level.

ONIOM Calculations on Wild-Type OSC. The proposed mechanism of OSC (Scheme 1) was subsequently studied using QM/MM (ONIOM) methodology. The QM/MM method has been employed in a number of mechanistic studies on enzymes.[35−37] In a recent QM/MM study by Rajamani et al.,[21] the catalytic mechanism of SHC, a related enzyme, was systematically analyzed. The two major findings were 1) the proposed ring expansion process from initial 5-membered to 6-membered ring is unlikely for either C- or D-ring formation, instead 6-membered ring is formed directly; 2) the distribution of two key products, the 6,6,6,5-tetracyclic carbon skeleton and the 6,6,6,6,5-pentacyclic hopanoids, is controlled by kinetics.[21] In the current study on OSC, we are interested in the product specificity at the hydride/methyl-shifting stage after the formation of the 6,6,6,5-tetracyclic intermediate **4**. Intermediates **1**−**8** and the TSs linking these were thus optimized by using ONIOM calculations (Scheme 1). As mentioned above, His232 was set to the HID protonation isomer (Figure 1).

dx.doi.org/10.1021/jp3091396 | J. Phys. Chem. B 2012, 116, 13857−13862

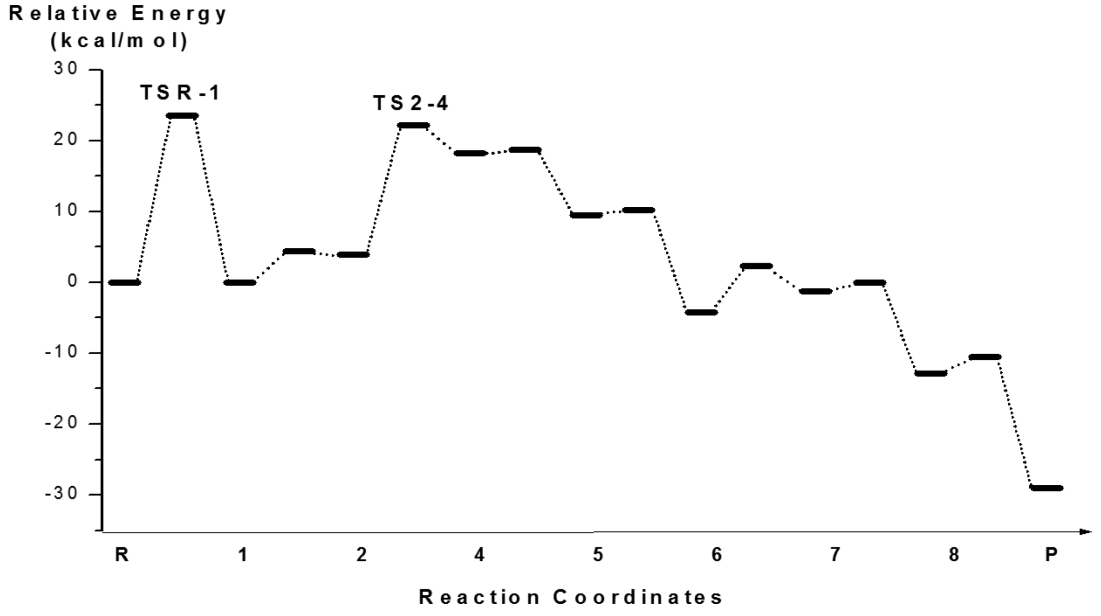

Figure 1. Energy profile of the proposed mechanism of the wild-type OSC (H232 is in the HID form).

The first step is the protonation of **R**, which is concerted with A ring formation, to give **1**. As this step has the highest barrier in the catalytic process (23.0 kcal/mol), we suggest that it is the rate-limiting step of OSC. It should be noted that the obtained barrier height 23.0 kcal/mol is much lower than a previous small model QM study[15] (40 kcal/mol with B3LYP/BS1). The optimized geometry of **TSR-1** is shown in Figure 2a. The B-ring formation is relatively easy, whereby intermediate **2** is obtained. The 6,6,6-tricyclic intermediate **3** was found to be unstable, which is consistent with the previous QM/MM study on SHC[21] as well as the fact that 6,6,6-tricyclic products are never observed. The optimized geometry of **TS2−4** is shown in Figure 2b. It should be mentioned that in SHC, the C-ring formation may lead to 6,6,5-tricyclic, 6,6,6,5-tetracyclic and 6,6,6,6,5-pentacyclic intermediates. In the current study on OSC, 6,6,5-tricyclic and 6,6,6,6,5-pentacyclic intermediates were not considered, as our focus is on the product specificity at the hydride/methyl-shifting stage. The conversion of **4** to **8** is fast and exothermic (Figure 1), whereafter **8** converts to lanosterol.

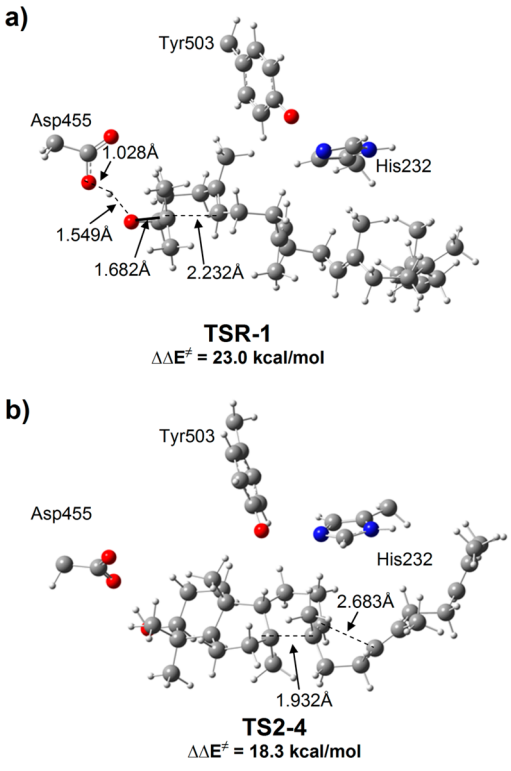

Figure 2. Optimized geometries of (a) **TSR-1** and (b) **TS2-4**.

ONIOM Calculations on OSC Mutants. Intermediate **8** is the most stable one of those shown in Scheme 1 (Figure 1), which seems to support the hypothesis that product specificity of OSC is achieved by the stabilization of the cationic intermediates.[5,11−14,16] However, our QM and QM/MM calculations show that intermediate **9**, which is the precursor of Parkeol (**P2**), is more stable than **8** (the precursor of **P1**). The relative energies of key intermediates **6**, **8**, and **9** in the wild-type OSC and those in the H232S and H232T mutants were thus compared (Table 3, columns 2, 5, and 6). The trends of the relative energies of these intermediates are the same. The relative energies of the three products in different mutants were also studied, and the results show that **P2** is more stable than **P1** (Table 3). Hence, according to our calculations, **P2** is

Table 3. Relative Energies of the Key Intermediates and Products in the QM/MM Calculations

intermediates or products	relative energy[a]				
	wild-type HID	H232S	H232T	wild-type HIE	wild-type HIP
6	24.5	22.3	25.5	24.0	26.0
8	16.0	13.6	17.0	15.7	16.3
9	12.1	10.4	13.3	11.8	13.0
P1	0.0	0.0	0.0	0.0	0.0
P2	−6.6	−4.1	−5.3	−5.0	−7.0
P3	1.5	10.0	6.2	4.7	0.8

[a]ONIOM-EE(B3LYP/BS2:AMBER) energies, relative to P1, in kcal/mol.

dx.doi.org/10.1021/jp3091396 | J. Phys. Chem. B 2012, 116, 13857−13862

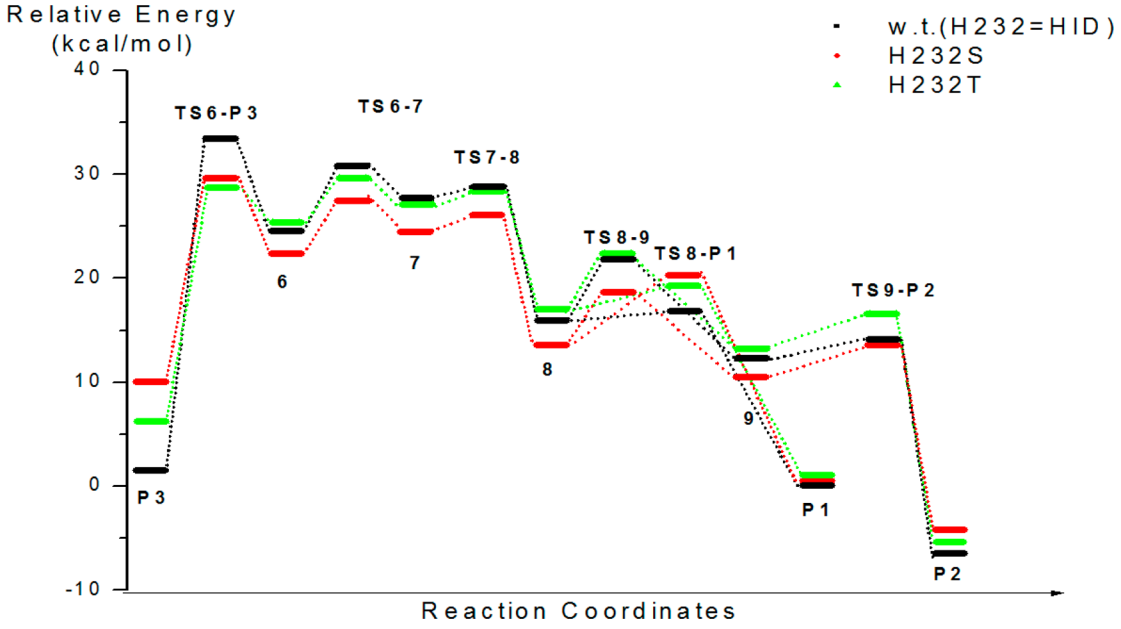

Figure 3. Energy profiles of wild-type OSC (in black), H232S (in red), and H232T (in green) mutants.

thermodynamically more favorable than **P1** for all the systems investigated in this study.

In the previous QM/MM study by Rajamani et al.,[21] the product specificity of SHC was found to be controlled by kinetics. We thus investigate whether this holds true also for OSC. In the current work, only the barrier heights for the conversions in the last few steps were studied, in order to explain why **P1**, **P2**, and **P3** are selectively generated in wild-type OSC, H232S, and H232T mutants, respectively (Table 4 and Figure 3). In the wild-type OSC and the H232S mutant, the formation of **7** is faster than **P3** (Table 4 and Figure 3), and thus **P3** is not generated. In the H232T mutant, however, the barrier for formation of **P3** is lower than that leading to formation of **7** (Table 4 and Figure 3). This hence explains why **P3** is the product in the H232T mutant. Similarly, in wild-type OSC, as the formation of **P1** from **8** is faster than the formation of **9** (Table 4 and Figure 3), **P1** is the preferred product, although **P2** is thermodynamically more stable.

Table 4. Barrier Heights for the Key Conversions That Determine Product Specificity

	barrier heights[a]				
conversion	wild-type HID	H232S	H232T	wild-type HIE	wild-type HIP
6→7	6.4	5.3	4.3	5.5	4.2
6→P3	9.0	7.2	3.3	6.5	7.3
8→9	5.8	5.0	5.5	5.2	6.6
8→P1	0.8	6.6	2.2	4.3	5.3
9→P2	2.0	3.1	3.4	5.6	7.2

[a]ONIOM-EE(B3LYP/BS2:AMBER) energies, in kcal/mol.

For the H232S mutant, finally, the reaction from **8** to **9** is associated with a lower barrier than **8** to **P1**, which thus in this case, allows the system to proceed toward the observed product **P2**.

CONCLUSIONS

The catalytic mechanism and the product specificity of OSC were investigated using QM/MM calculations. The first step, i.e. protonation of the epoxide ring of oxidosqualene, was found to be rate-limiting. According to our DFT and ONIOM calculations, intermediate **9**, which is the precursor of parkeol, is more stable than **8** (the precursor of lanosterol). Therefore, we suggest that the relative stability of the cationic intermediates may to some extent contribute to the OSC product specificity, but is not the main factor governing this. The barrier heights at the hydride/methyl-shifting stage were found to be consistent with the product profiles of different OSC mutants. Hence, we suggest that the product specificity of OSC is likely to be controlled by kinetics. Mutagenesis results in changes of the electrostatic environment of the enzyme, and thus affects the reaction barriers at the hydride/methyl-shifting stage. When the base group deprotonates the carbon cation intermediate, the product is generated irreversibly.

ASSOCIATED CONTENT

Supporting Information

Illustration of HID, HIE, and HIP models; AMBER parameters for lanosterol; Cartesian coordinates (QM reigion) and QM/MM energies of key intermediates and TS; Complete citation for ref 28. This material is available free of charge via the Internet at http://pubs.acs.org.

AUTHOR INFORMATION

Corresponding Author

*E-mail: leif.eriksson@chem.gu.se.

Notes

The authors declare no competing financial interest.

ACKNOWLEDGMENTS

The National University of Ireland-Galway and the Faculty of Science of the University of Gothenburg are gratefully acknowledged for financial support. The SFI/HEA Irish Centre

for High-End Computing (ICHEC) is acknowledged for the provision of computational facilities and support.

REFERENCES

(1) Nes, W. D. *Chem. Rev.* **2011**, *111*, 6423−6451.
(2) Huff, M. W.; Telford, D. E. *Trends Pharmacol. Sci.* **2005**, *26*, 335−340.
(3) Thoma, R.; Schulz-Gasch, T.; D'Arcy, B.; Benz, J.; Aebi, J.; Dehmlow, H.; Hennig, M.; Stihle, M.; Ruf, A. *Nature* **2004**, *432*, 118−122.
(4) Barth, M. M.; Binet, J. L.; Thomas, D. M.; deFornel, D. C.; Samreth, S.; Schuber, F. J.; Renaut, P. P. *J. Med. Chem.* **1996**, *39*, 2302−2312.
(5) Wu, T.-K.; Liu, Y.-T.; Chang, C.-H.; Yu, M.-T.; Wang, H.-J. *J. Am. Chem. Soc.* **2006**, *128*, 6414−6419.
(6) Wu, T.-K.; Chang, Y.-C.; Liu, Y.-T.; Chang, C.-H.; Wen, H.-Y.; Li, W.-H.; Shie, W.-S. *Org. Biomol. Chem.* **2011**, *9*, 1092−1097.
(7) Wu, T.-K.; Chang, C.-H.; Wen, H.-Y.; Liu, Y.-T.; Li, W.-H.; Wang, T.-T.; Shie, W.-S. *Org. Lett.* **2010**, *12*, 500−503.
(8) Wu, T.-K.; Li, W.-H.; Chang, C.-H.; Wen, H.-Y.; Liu, Y.-T.; Chang, Y.-C. *Eur. J. Org. Chem.* **2009**, 5731−5737.
(9) Wu, T.-K.; Wen, H.-Y.; Chang, C.-H.; Liu, Y.-T. *Org. Lett.* **2008**, *10*, 2529−2532.
(10) Wu, T.-K.; Wang, T.-T.; Chang, C.-H.; Liu, Y.-T.; Shie, W.-S. *Org. Lett.* **2008**, *10*, 4959−4962.
(11) Wu, T.-K.; Liu, Y.-T.; Chiu, F.-H.; Chang, C.-H. *Org. Lett.* **2006**, *8*, 4691−4694.
(12) Wu, T. K.; Yu, M. T.; Liu, Y. T.; Chang, C. H.; Wang, H. J.; Diau, E. W. G. *Org. Lett.* **2006**, *8*, 1319−1322.
(13) Wu, T. K.; Liu, Y. T.; Chang, C. H. *Chembiochem* **2005**, *6*, 1177−1181.
(14) Wu, T. K.; Chang, C. H. *Chembiochem* **2004**, *5*, 1712−1715.
(15) Gao, D. Q.; Pan, Y. K.; Byun, K.; Gao, J. L. *J. Am. Chem. Soc.* **1998**, *120*, 4045−4046.
(16) Kürti, L.; Chein, R.-J.; Corey, E. J. *J. Am. Chem. Soc.* **2008**, *130*, 9031−9036.
(17) Matsuda, S. P. T.; Wilson, W. K.; Xiong, Q. B. *Org. Biomol. Chem.* **2006**, *4*, 530−543.
(18) Hess, B. A.; Smentek, L. *Mol. Phys.* **2004**, *102*, 1201−1206.
(19) Hess, B. A.; Smentek, L. *Org. Lett.* **2004**, *6*, 1717−1720.
(20) Hess, B. A. *Eur. J. Org. Chem.* **2004**, 2239−2242.
(21) Rajamani, R.; Gao, J. L. *J. Am. Chem. Soc.* **2003**, *125*, 12768−12781.
(22) Hess, B. A. *Org. Lett.* **2003**, *5*, 165−167.
(23) Jenson, C.; Jorgensen, W. L. *J. Am. Chem. Soc.* **1997**, *119*, 10846−10854.
(24) Becke, A. D. *J. Chem. Phys.* **1993**, *98*, 5648−5652.
(25) Lee, C. T.; Yang, W. T.; Parr, R. G. *Phys. Rev. B* **1988**, *37*, 785−789.
(26) Becke, A. D. *Phys. Rev. A* **1988**, *38*, 3098−3100.
(27) Zhao, Y.; Truhlar, D. G. *Theor. Chem. Acc.* **2008**, *120*, 215−241.
(28) Frisch, M. J.; Trucks, G. W.; Schlegel, H. B.; Scuseria, G. E.; Robb, M. A.; Cheeseman, J. R.; Scalmani, G.; Barone, V.; Mennucci, B.; Petersson, G. et al.*Gaussian 09, Revision A.02*; Gaussian, Inc.: Wallingford CT, 2009.
(29) *Molecular Operating Environment, MOE*; Chemical Computing Group Inc.: Montreal, Canada; http://www.chemcomp/com.
(30) Tian, B. X.; Eriksson, L. A. *J. Phys. Chem. B* **2011**, *115*, 13003−13011.
(31) Vreven, T.; Byun, K. S.; Komaromi, I.; Dapprich, S.; Montgomery, J. A.; Morokuma, K.; Frisch, M. J. *J. Chem. Theory Comput.* **2006**, *2*, 815−826.
(32) Duan, Y.; Wu, C.; Chowdhury, S.; Lee, M. C.; Xiong, G. M.; Zhang, W.; Yang, R.; Cieplak, P.; Luo, R.; Lee, T.; Caldwell, J.; Wang, J. M.; Kollman, P. *J. Comput. Chem.* **2003**, *24*, 1999−2012.
(33) Wang, J. M.; Wang, W.; Kollman, P. A.; Case, D. A. *J. Mol. Graph.* **2006**, *25*, 247−260.
(34) Wang, J. M.; Wolf, R. M.; Caldwell, J. W.; Kollman, P. A.; Case, D. A. *J. Comput. Chem.* **2004**, *25*, 1157−1174.
(35) Shaik, S.; Cohen, S.; Wang, Y.; Chen, H.; Kumar, D.; Thiel, W. *Chem. Rev.* **2010**, *110*, 949−1017.
(36) Senn, H. M.; Thiel, W. *Curr. Opin. Chem. Biol.* **2007**, *11*, 182−187.
(37) Garcia-Viloca, M.; Gao, J.; Karplus, M.; Truhlar, D. G. *Science* **2004**, *303*, 186−195.